DOI: 10.1002/ejic.200901099

Syntheses and Physicochemical Properties of Low-Melting Salts Based on VOF_4^- and $MoOF_5^-$, and the Molecular Geometries of the Dimeric $(VOF_4^-)_2$ and $Mo_2O_4F_6^{2-}$ Anions

Takatsugu Kanatani,[a] Kazuhiko Matsumoto,[a] and Rika Hagiwara*[a]

Keywords: Ionic liquids / Fluorides / Vanadium / Molybdenum / Structure elucidation

1-Ethyl-3-methylimidazolium ($EMIm^+$) and *N*-butylpyridinium (BPy^+) salts of the oxotetrafluorovanadate (VOF_4^-) and oxopentafluoromolybdate ($MoOF_5^-$) anions with low melting temperatures have been synthesized by the reactions of the corresponding fluorohydrogenate ionic liquids and metal oxide fluoride. Differential scanning calorimetry reveals that the melting points of $EMImVOF_4$, $BPyVOF_4$, and $BPyMoOF_5$ are 348, 346, and 346 K, respectively, whereas the room-temperature ionic liquid $EMImMoOF_5$ only exhibits a glass transition at 190 K. Density, viscosity, and ionic conductivity of $EMImMoOF_5$ are 1.76 g cm^{-1}, 86 cP, and 5.1 mS cm^{-1} at 298 K, respectively. The cathode and anode limits of $EMImMoOF_5$ are –0.3 and +1.4 V (vs. Ag^+/Ag), respectively. The molecular geometries of the VOF_4^- and $Mo_2O_4F_6^{2-}$ anions have been determined by single-crystal X-ray diffraction, the latter being obtained by the hydrolysis of $MoOF_5^-$. The two VOF_4^- anions in $EMImVOF_4$ interact with each other through two highly asymmetric V–F···V bridges with V–F and V···F distances of 1.8633(7) and 2.3786(7) Å, respectively. A dinuclear anion in $(BPy)_2Mo_2O_4F_6$ possesses two symmetric Mo–F–Mo bonds with Mo–F lengths of 2.1691(12) and 2.1829(11) Å.

Introduction

Transition-metal oxide fluorides and their anionic derivatives have attracted more and more attention for their unique properties[1] such as magnetism,[2] luminescence,[3] and catalysis.[4–6] Vanadium gives a variety of oxofluoroanions at different oxidation states, which have potential applications in catalytic and medicinal chemistry,[7–10] including $V^{IV}OF_3^-$,[11] $V^{IV}OF_4^{2-}(OH_2)$,[12–14] $V^{IV}_2O_2F_8^{4-}$,[15,16] $V^{IV}OF_5^{3-}$,[17] $V^{V}OF_4^-$,[18–20] $V^{V}OF_5^{2-}$,[21] $V^{V}O_2F_3^{2-}$,[22] and $V^{V}_2O_4F_5^{3-}$.[23] A recent spectroscopic study combined with a DFT calculation characterized the monomeric VOF_4^- anion in its tetramethylammonium salt,[20] whereas the VOF_4^- anion determined in $CsVOF_4$ has a secondary contact from a neighboring anion, resulting in a chain-like anionic unit.[19] Molybdenum also forms oxofluoro complex anions in diverse coordination states including $Mo^{V}OF_5^{2-}$,[24,25] $Mo^{V}_2O_2F_9^{3-}$,[25] $Mo^{VI}OF_5^-$,[26,27] $Mo^{VI}O_2F_4^{2-}$,[28] $Mo^{VI}_2O_6F_3^{3-}$,[25,29] and $Mo^{VI}_4O_{12}F_2^{2-}$,[30] where some of the anions provide interesting structures with unique bridging states. Molecular units structurally related to these anions were also reported.[31]

The present study describes the syntheses and the physicochemical and structural properties of 1-ethyl-3-methylimidazolium ($EMIm^+$) and *N*-butylpyridinium (BPy^+) salts of VOF_4^- and $MoOF_5^-$. The two cations, $EMIm^+$ and BPy^+, often give low-temperature melting salts, sometimes classified into ionic liquids (ILs), which have potential applications such as electrolytes and reaction media owing to their unique properties including nonflammability, negligible vapor pressure, wide liquid-phase temperature range, and high chemical and electrochemical stability. ILs based on transition-metallate anions are attracting considerable attention as alternative media for homogeneous and heterogeneous reactions catalyzed by the transition metals.[32–38] In our previous study, a series of $EMIm^+$, BPy^+, and *N*-alkyl-*N*-methylpyrrolidinium salts of BF_4^-, PF_6^-, AsF_6^-, SbF_6^-, NbF_6^-, TaF_6^-, UF_6^-, and WF_7^- were prepared by the fluoroacid–base reactions between fluorohydrogenate ILs containing the corresponding cations and metal fluorides.[39–42] An IL based on WOF_5^-, $EMImWOF_5$, was also prepared by hydrolysis of $EMImWF_7$ or the acid–base reaction using WOF_4.[43] The present attempt to prepare ILs based on VOF_4^- and $MoOF_5^-$ is an interesting research subject for structural analysis of the anionic species as well as the applications in catalytic chemistry as described above. The single-crystal structure of the related compound $(BPy)_2Mo_2O_4F_6$ is also reported.

[a] Department of Fundamental Energy Science, Graduate School of Energy Science, Kyoto University,
Sakyo-ku, Kyoto 606-8501, Japan
Fax: +81-75-753-5906
E-mail: hagiwara@energy.kyoto-u.ac.jp

Supporting information for this article is available on the WWW under http://dx.doi.org/10.1002/ejic.200901099.

Results and Discussion

Syntheses of VOF_4^- and $MoOF_5^-$ Salts

Scheme 1 shows the structures of the cations of the salts and the reaction procedure used in this study. The acid–base reaction between the fluorohydrogenate IL and fluoride ion acceptor, VOF_3 or $MoOF_4$, is exothermic and a rise in vapor pressure of HF was observed upon the addition of the oxide fluoride. Removal of the HF byproduct gives a yellow solid for the VOF_4 salts, yellowish liquid for $EMImMoOF_5$, and colorless solid for $BPyMoOF_5$ at 298 K. In the previous study,[39] attempts to prepare $EMImVF_6$ or $EMImMoF_7$ by the reaction of $EMIm(FH)_{2.3}F$ and VF_5 or MoF_6 failed due to the strong oxidizing power of the metal fluoride. On the other hand, VOF_3 and $MoOF_4$ are moderate enough precursors to prepare the $EMIm^+$ and BPy^+ salts in the present method. The stoichiometric reactions proceeded and no byproducts other than HF were observed in any case. Vibrational spectra of the obtained salts at room temperature are given in Figures S1–S8 (Supporting Information). The characteristic V=O stretching mode is observed at around 1010 cm^{-1} in the Raman and IR spectra of $EMImVOF_4$ and $BPyVOF_4$,[18] which agrees well with the reported values for the V=O stretching modes including the chain-like VOF_4^- in $CsVOF_4$.[18,19] Since the vibrational frequencies observed for VOF_4^- in liquid $EMImVOF_4$ at 350 K are close to those in solid $EMImVOF_4$ at room temperature, the dimeric anion observed in the solid state (see below) probably remains in the liquid state (Figure S3, Supporting Information) at 350 K. The Mo=O stretching mode is observed at around 970 cm^{-1} in the Raman and IR spectra of $EMImMoOF_5$ and $BPyMoOF_5$ as in the cases of the other salts containing the discrete $MoOF_5^-$ anions.[27]

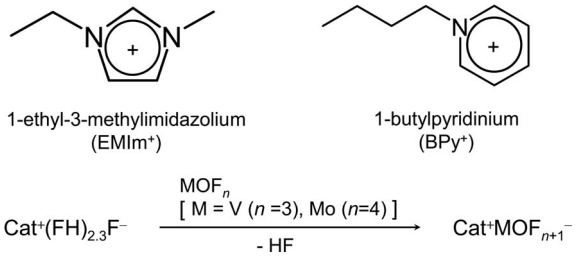

Scheme 1. The structures of the cations used and the procedure for the syntheses of the present salts.

Physicochemical and Electrochemical Properties

Physicochemical properties of $EMImVOF_4$, $BPyVOF_4$, $EMImMoOF_5$, and $BPyMoOF_5$ are listed in Table 1, and those reported previously for $EMImWOF_5$ are also listed for comparison.[43] Figure 1 shows the DSC curves for the present four salts. While $EMImVOF_4$, $BPyVOF_4$, and $BPyMoOF_5$ exhibit endothermic peaks assigned to melting in the range between 346 and 348 K during the heating process, $EMImMoOF_5$ exhibits only a glass transition at 190 K and forms a room-temperature IL. The melting points observed for the present VOF_4 salts are relatively high compared to the other $EMIm^+$ or BPy^+ salts of a monovalent anion, which is probably due to the formation of a dimeric unit as described below. The molar volumes of $EMImMoOF_5$ (183 $cm^3 mol^{-1}$) and $EMImWOF_5$ (180 $cm^3 mol^{-1}$) calculated from their densities and formula weight are close to each other due to the similar sizes of Mo and W. In the Walden plot where the logarithmic reciprocal molar conductivities of ILs composed of dialkylimidazolium cations and fluoroanions are plotted against their logarithmic viscosities, the value for $EMImMoOF_5$ does not deviate from the general trend (Figure S9, Supporting Information). This suggests that the mechanism of diffusion of the ionic species in $EMImMoOF_5$ is similar to the other ILs and that the viscosity dominates the ionic conductivity.

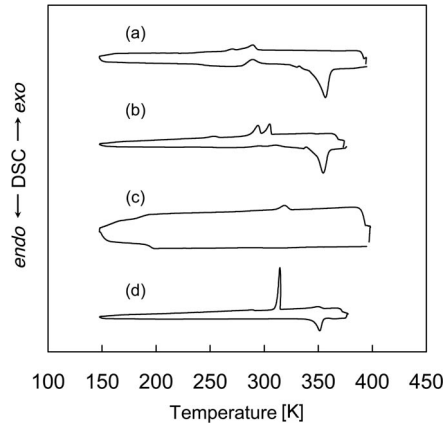

Figure 1. DSC curves for (a) $EMImVOF_4$, (b) $BPyVOF_4$, (c) $EMImMoOF_5$, and (d) $BPyMoOF_5$.

Figure 2 shows the cyclic voltammogram of a glassy carbon electrode in $EMImMoOF_5$ at 298 K. The cathode and anode limits were determined as the potential of a

Table 1. Thermal and physicochemical properties[a] of the present salts measured.

	[EMIm][VOF_4]	[BPy][VOF_4]	[EMIm][$MoOF_5$]	[BPy][$MoOF_5$]	[EMIm][WOF_5][b]
MW	254	279	318	343	406
ρ [g cm^3]	–	–	1.76	–	2.25
T_m [K]	348	346	–	346	253
T_g [K]	243	249	190	n.d.	182
T_d [K]	423	477	509	570	–
η [cP]	–	–	86	–	105
σ [mS cm^{-1}]	–	–	5.1	–	3.0

[a] MW: molecular weight, T_m: melting point, T_g: glass transition temperature, T_d: decomposition temperature (T_d is the temperature at the 5% loss of the total weight), ρ: density at 298 K, η: viscosity at 298 K, σ: ionic conductivity at 298 K, n.d.: not detected. [b] Ref.[43]

glassy carbon electrode, where the absolute values of the current densities exceeded 0.5 mA cm^{-2} during cyclic voltammetry at a scan rate of 10 mV s^{-1}. The cathode limit is –0.3 V vs. Ag^+/Ag and is assigned to the reduction of the anion, because the reduction of $EMIm^+$ is observed around –3.0 V vs. Ag^+/Ag.[44] The anode limit is +1.4 V vs. Ag^+/Ag, which is ascribed to the oxidative decomposition of the cation, similar to the cases of other ILs based on fluoro complex anions.[39]

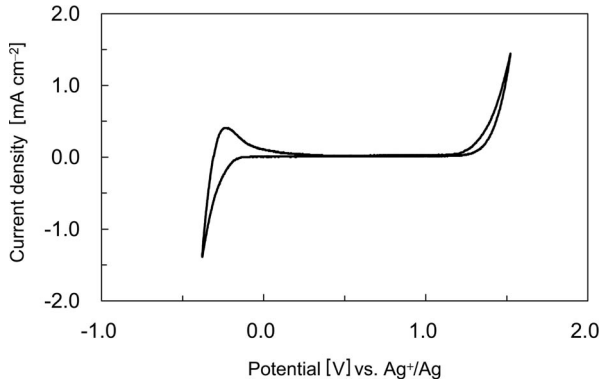

Figure 2. Cyclic voltammogram of a glassy carbon electrode in $EMImMoOF_5$ at room temperature.

Crystal Structures of $EMImVOF_4$ and $(BPy)_2Mo_2O_4F_6$

Selected bond lengths and angles are listed in Table 2. Geometries of the interactions between the hydrogen atoms in the cation and fluorine or oxygen atoms in the anion (H···F or H···O < the sum of van der Waals distances of 2.7 Å) are listed in Table S1 (Supporting Information). The monoclinic lattice of $EMImVOF_4$ contains one pair of ions in the asymmetric unit. The ORTEP diagram of the asymmetric unit is shown in Figure 3a. Typical bond lengths and bond angles are observed for the $EMIm^+$ cation in $EMImVOF_4$.[39] The C7 atom is sticking out of the imidazolium ring plane with a C2–N3–C6–C7 torsion angle of –100.64(14)°. Two VOF_4^- anions interact with each other in $EMImVOF_4$ through two asymmetric F–V···F bridging bonds (Figure 3b). The V···F contact of 2.3786(7) Å is longer than the terminal V–F bond lengths in the range between 1.7883(8) and 1.8633(7) Å and is regarded as a weak interaction. On the basis of the deformation from a trigonal bipyramid molecular geometry, the V=O double bond repels the two axial fluorine atoms away from the oxygen atom, whereas the fluorine atom provided by the other VOF_4^- (F4a) slightly repels the two equatorial fluorine atoms (O–V–F angles in the 99–104°). The two repulsions result in the nearly square pyramidal structure of the VOF_4^- unit with the oxygen atom on the top. The *trans*-O1–V···F4a angle is nearly linear [173.15(5)°]. The V1–F4 bond length of 1.8633(7) Å is longer than the other three terminal V–F bonds [1.8055(7), 1.7883(8), and 1.8242(7) Å], as F4 contributes to the secondary contact to the other vanadium atom. The only crystallographically determined example of VOF_4^- previously is the one in $CsVOF_4$, where VOF_4^- forms an infinite chain through a weak V···F contact [2.312(10) Å].[19] The V···F contact distance in $EMImVOF_4$ is similar to that in $CsVOF_4$, and the overall coordination states around the vanadium atom in these two salts are close to each other. Both the V=O and V–F bond lengths in $EMImVOF_4$ are shorter than those in the V^{IV} oxofluoroanions such as the dimeric $V_2O_2F_8^{4-}$ anion in $C_2H_4(NH_2C_2H_4NH_3)_2V_2O_2F_8$, where the terminal V=O length is 1.611(3) Å and the terminal V–F bond lengths ranges from 1.917(2) to 1.973(3) Å.[15] The V–F–V bridge is asymmetric as in the case for $EMImVOF_4$, where the difference in the two V–F bond lengths is smaller [1.969(2) and 2.157(2) Å for $C_2H_4(NH_2C_2H_4NH_3)_2V_2O_2F_8$ and 1.8633(7) and 2.3786(7) Å for $EMImVOF_4$]. The bond valence sum analysis revealed that the vanadium atom of VOF_4^- in $EMImVOF_4$ has a total bond valence of 4.831 without taking the weak V···F contact into account,[45,46] whereas the contribution of the weak V···F contact slightly increases the total bond valence to 4.995. The total bond valence for the vanadium(IV) atom in $V_2O_2F_8^{4-}$ is 3.96.[15] Therefore, both the vanadium atoms in the VOF_4^- and $V_2O_2F_8^{4-}$ anions are consistent with their oxidation states, whereas the difference in the bridging forms probably arises from the more crowded coordination environment around the vanadium atom at the oxidation state of five. The anions in $EMImVOF_4$ behave like a doubly charged anion in $EMImVOF_4$, which probably results in the relatively high melting point of $EMImVOF_4$. The packing diagram of $EMImVOF_4$ along the *a* axis is shown in Figure 4. The fluorine atoms in VOF_4^- mainly interact with the ring protons, whereas some alkyl protons also have short contacts with the fluorine atoms (Table S1, Supporting Information).

Table 2. Selected bond lengths and bond angles for the anions of $EMImVOF_4$ and $(BPy)_2Mo_2O_4F_6$.

The VOF_4^- anion of $EMImVOF_4$			
V1–O1	1.5745(10)	F1–V1–F2	89.57(4)
V1–F1	1.8055(7)	F1–V1–F3	162.37(3)
V1–F2	1.7883(8)	F1–V1–F4	87.65(3)
V1–F3	1.8242(7)	F2–V1–F3	87.91(4)
V1–F4	1.8633(7)	F2–V1–F4	154.55(4)
V1···F4a	2.3786(7)	F3–V1–F4	87.16(3)
		O1–V1···F4a	173.15(5)
O1–V1–F1	99.03(4)	F1–V1···F4a	81.98(3)
O1–V1–F2	103.64(5)	F2–V1···F4a	83.12(3)
O1–V1–F3	98.52(4)	F3–V1···F4a	80.40(3)
O1–V1–F4	101.78(5)	F4–V1···F4a	71.44(3)
The $MoO_2F_3^-$ anion of $(BPy)_2Mo_2O_4F_6$			
Mo1–O1	1.6920(16)	O2–Mo1–F1	97.57(8)
Mo1–O2	1.6874(16)	O2–Mo1–F2	96.13(7)
Mo1–F1	1.9083(13)	O2–Mo1–F3	93.70(7)
Mo1–F2	1.9280(11)	O2–Mo1–F3a	163.27(7)
Mo1–F3	2.1691(12)	F1–Mo1–F2	157.71(5)
Mo1–F3a	2.1829(11)	F1–Mo1–F3	80.66(5)
		F1–Mo1–F3a	80.21(5)
O1–Mo1–O2	104.30(8)	F2–Mo1–F3	80.99(5)
O1–Mo1–F1	97.98(7)	F2–Mo1–F3a	81.61(5)
O1–Mo1–F2	95.55(7)	F3–Mo1–F3a	69.57(5)
O1–Mo1–F3	161.96(7)	Mo1–F3–Mo1	110.43(5)
O1–Mo1–F3a	92.43(6)		

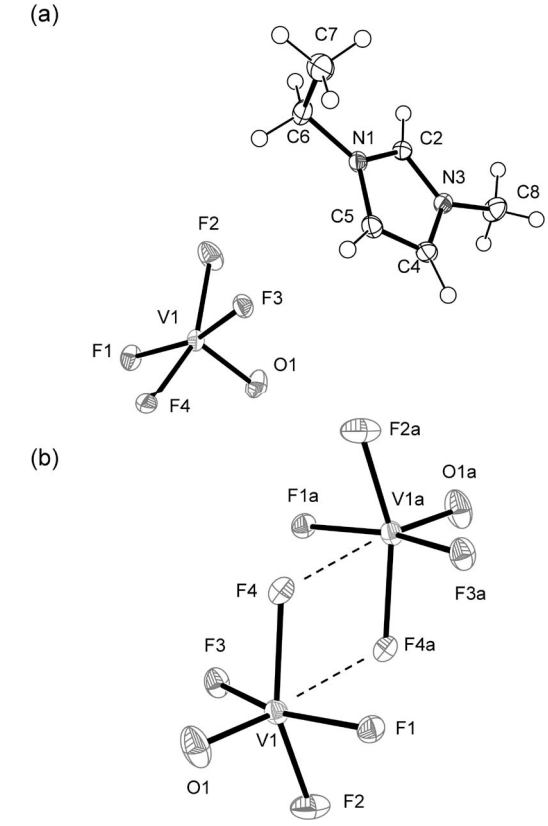

Figure 3. The ORTEP diagram of (a) the asymmetric unit and (b) the $(VOF_4^-)_2$ unit in $EMImVOF_4$.

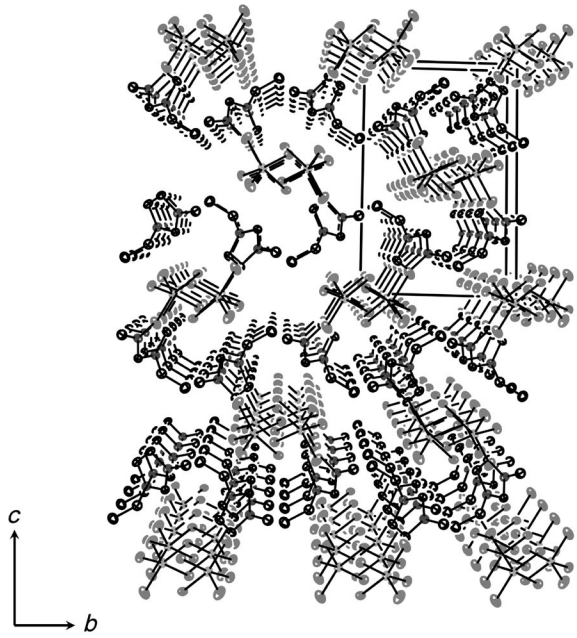

Figure 4. The perspective view of the molecular packing in $EMImVOF_4$.

The hydrogen atoms are omitted for clarity. Single crystals of $(BPy)_2Mo_2O_4F_6$ were accidentally obtained by hydrolysis with a trace of water in the solvent during the crystal growth of $BPyMoOF_5$. The X-ray diffraction powder pattern of $BPyMoOF_5$ was different from the pattern of $(BPy)_2Mo_2O_4F_6$ calculated from the single-crystal X-ray structure described below, which suggest the original $BPyMoOF_5$ sample does not contain $(BPy)_2Mo_2O_4F_6$ (Figure S10, Supporting Information). The ORTEP diagram of the asymmetric unit is shown in Figure 5a. The expected geometrical parameters[47,48] are observed for the BPy^+ cation determined in $(BPy)_2Mo_2O_4F_6$. Whereas the C7–C8–C9–C10 angle [178.87(17)°] adopts a nearly *anti* conformation, the N1–C7–C8–C9 torsion angle is –63.8(2)° because of the effect of crystal packing.

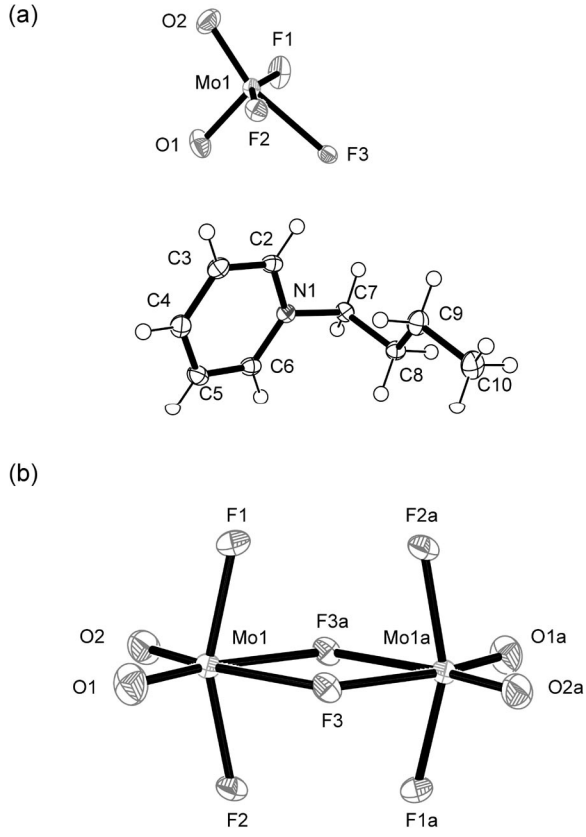

Figure 5. The ORTEP diagram of (a) the asymmetric unit and (b) the dinuclear $Mo_2O_4F_6^{2-}$ anion in $(BPy)_2Mo_2O_4F_6$.

In the $Mo_2O_4F_6^{2-}$ anion, the four Mo–F bridging bond lengths are nearly the same [2.1691(12) and 2.1829(11) Å; Figure 5b]. Similar bridging bond lengths are observed in the anionic dinuclear Mo^{VI} species $Mo_2O_6F_3^{3-}$ in $[Cu^{II}(3\text{-apy})_4]_3(Mo_2O_6F_3)_2$ that is made up of two face-sharing octahedral with three F bridging bonds [2.181(2) and 2.113(2) Å].[29] Another example of molybdenum complex anion containing Mo–F–Mo is $Mo^{V}_2O_2F_9^{3-}$, where the Mo–F bridging bonds range from 2.118(2) to 2.19(2) Å.[25] The terminal Mo–F [1.9083(13) and 1.9280(11) Å] and Mo=O [1.6920(16) and 1.6874(16) Å] bond lengths in $Mo_2O_4F_6^{2-}$ agree well with the values in the known Mo^{VI} species.[29,30] The two oxygen atoms occupy a *cis* position with each other, and the order in bond angle of *cis*-F–Mo–F [81.61(5)–69.57(5)°] < *cis*-F–Mo–O [97.98(7)–92.43(6)] < *cis*-O–Mo–O [104.30(8)] satisfies the valence shell electron

pair repulsion theory. The very similar structural unit $Mo_2O_6F_4$ was observed in $\{[Ni_3(tpyprz)_2(H_2O)_2](Mo_5O_{15})(Mo_2F_2O_4)[O_3P(CH_2)_3PO_3]_2\}\cdot 8H_2O$, where two terminal fluorine atoms are replaced by two oxygen atoms from propylenediphosphonate tethers of the chain.[31] The unusually small F3–Mo–F3a angle of 69.57(5)° is due to the long Mo–F3 and Mo–F3a contacts. The packing diagram of $(BPy)_2Mo_2O_4F_6$ is shown in Figure 6. A hydrophobic region is formed between the two butyl groups from two adjacent cations. The dinuclear $Mo_2O_4F_6^{2-}$ anion also has a 1D column by the electrostatic interactions between the cations and anions.

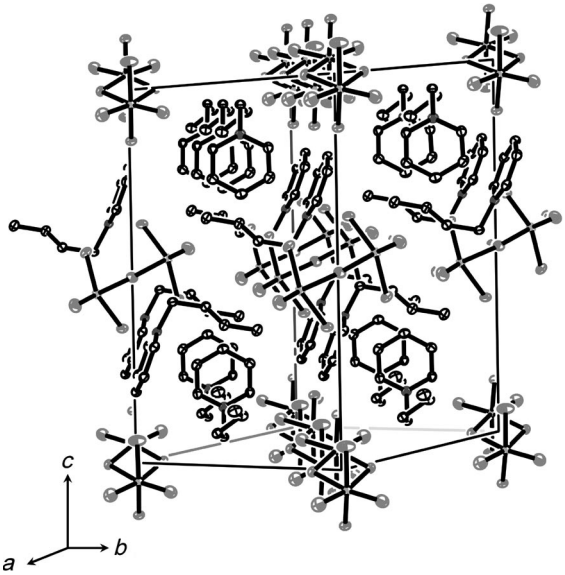

Figure 6. Perspective view of the molecular packing in $(BPy)_2Mo_2O_4F_6$. The hydrogen atoms are omitted for clarity.

Conclusions

In this paper, the syntheses and physicochemical properties of novel $EMIm^+$ and BPy^+ salts of VOF_4^- and $MoOF_5^-$ were described. Although only $EMImMoF_5$ forms a room-temperature IL (viscosity of 86 cP and conductivity of 5.1 mS cm^{-1}), the other three salts also show low melting points (346–348 K). The cathode and anode limits of $EMImMoOF_5$ in electrochemical window measurements are at –0.3 and +1.4 V (vs. Ag^+/Ag), respectively, where the cathode limit is assigned to the reduction of the anion. The molecular geometries of the VOF_4^- and $Mo_2O_4F_6^{2-}$ anions were determined by single-crystal X-ray diffraction, the latter being obtained by the hydrolysis of $MoOF_5^-$. The two VOF_4^- anions in the crystal structure of $EMImVOF_4$ interact with each other through two highly asymmetric V–F···V bridges. The dinuclear anion in the crystal structure of $(BPy)_2Mo_2O_4F_6$ possesses two symmetric Mo–F–Mo bonds.

Experimental Section

General: Moisture-sensitive materials were handled in a glove box under a dry Ar atmosphere. All reactions involving anhydrous HF (aHF, Daikin Industries, purity >99%) were performed in PFA (tetrafluoroethyleneperfluoroalkylvinyl ether copolymer) reactors. Anhydrous HF was dried with K_2NiF_6 (Ozark-Mahoning) for several days prior to use. The starting chlorides, EMImCl and BPyCl, were prepared by the reactions of the corresponding amine and chloroalkane.[49] The fluorohydrogenate salts were prepared by the reaction of the chloride and a large excess of anhydrous HF.[49] Vanadium oxide trifluoride (Aldrich, purity 99%) was used as supplied. Molybdenum oxide fluoride, $MoOF_4$, was synthesized by the reaction of a large excess of MoF_6 and H_2O by eliminating unreacted MoF_6 and byproduct HF at room temperature.

$EMImVOF_4$: Vanadium oxide trifluoride (4.28 mmol) loaded in one arm of a T-shaped PFA was slowly added onto $EMIm(FH)_{2.3}F$ (4.28 mmol) in the other arm at room temperature. After the addition of VOF_3, the obtained liquid was stirred for 4 h. A yellow powder sample was obtained after removal of liberated HF under dynamic vacuum at 340 K. Vibrational spectroscopy and elemental analysis identified the solid as $EMImVOF_4$. $C_6H_{14}F_4N_2OV$ (254.10): calcd. C 28.36, H 4.36, N 11.02; found C 28.49, H 4.27, N 11.14. Data for VOF_4^-: Raman (solid): $\tilde{\nu}$ = 1012 (m), 630 (m), 343 (s), 324 (w), 243 (m) cm^{-1}. Raman (liquid): $\tilde{\nu}$ = 1014 (m), 633 (m), 342 (s), 329 (w), 245 (m) cm^{-1}. IR: $\tilde{\nu}$ = 1012 (s), 629 (m), 600 (s) cm^{-1}. The following salts were prepared in the same manner as in the case of $EMImVOF_4$.

$BPyVOF_4$: $C_9H_{14}F_4NOV$ (279.15): calcd. C 38.72, H 5.06, N 5.02; found C 38.93, H 4.98, N 4.92. Data for VOF_4^-: Raman: $\tilde{\nu}$ = 1018 (m), 630 (m), 344 (s), 327 (w), 245 (m) cm^{-1}. IR: $\tilde{\nu}$ = 1013 (m), 625 (s), 592 (s) cm^{-1}.

$EMImMoOF_5$: $C_6H_{11}F_5MoN_2O$ (318.10): calcd. C 22.66, H 3.49, N 8.81; found C 22.82, H 3.42, N 8.83. Data for $MoOF_5^-$: Raman: $\tilde{\nu}$ = 968 (s), 661 (s), 316 (m) cm^{-1}. IR: $\tilde{\nu}$ = 972 (s), 663 (m, sh.), 490 (m) cm^{-1}.

$BPyMoOF_5$: $C_9H_{14}F_5MoNO$ (343.15): calcd. C 31.50, H 4.11, N 4.08; found C 31.56, H 4.36, N 4.09. Data for $MoOF_5^-$: Raman: $\tilde{\nu}$ = 971 (s), 661 (s), 302 (m) cm^{-1}. IR: $\tilde{\nu}$ = 958 (s), 655 (m, sh.), 621 (s), 490(m) cm^{-1}.

Spectroscopic Measurements: The Raman spectrum of $EMImVOF_4$ was obtained (LabRAM300, Horiba Jobin Yvon) by using the 632 nm line of a He–Ne laser as an excitation line at room temperature. Raman spectra of $BPyVOF_4$, $EMImMoOF_5$, and $BPyMoOF_5$ were recorded (FTS-175C, Bio-Rad Laboratories) by using the 1064 nm line of a Nd:YAG laser as the excitation line at room temperature. The samples for Raman spectroscopy were loaded in Pyrex test tubes. The IR spectra of solid and liquid samples were obtained by FTS-165 (BIO-RAD Laboratories). The samples were sandwiched between a pair of AgCl windows fixed in a stainless airtight cell.

Measurement of Physical and Electrochemical Properties: Differential scanning calorimetric analysis (DSC) was performed on the sample in an aluminum-sealed cell under dry Ar gas flow by using a Shimadzu DSC-60. The scanning rate of 10 K min^{-1} was used. Conductivity was measured by impedance technique with the aid of HZ-3000 electrochemical measurement system (Hokuto Denko). The cell for conductivity measurement was made of PFA and PTFE [poly(tetrafluoroethylene)] with platinum disk electrodes and was calibrated by a KCl standard aqueous solution. Viscosity was measured by a cone-plate rheometer DV-II + Pro (Brookfield Engineering Laboratories Inc.). The electrochemical window measurement was performed by using glassy carbon working and counter electrodes. The reference electrode was made of silver wire immersed in $EMImBF_4$ containing 0.05 M $AgBF_4$ separated from the electrolyte by a PTFE filter.

Single Crystal Growth: A mixture of acetonitrile and ethyl acetate saturated with $EMImVOF_4$ was loaded in one of the arms of a T-shaped PFA reactor, and then the end of the other tube was cooled by liquid nitrogen to transfer the solvent. The crystals which appeared in the PFA tube five days later were isolated by decanting the solution successively followed by the removal of the solvent under vacuum. Crystals selected in a glove box for X-ray diffraction were fixed in a quartz capillary (0.5 mm o.d., previously dried under a vacuum at 773 K) and sealed by using a micro oxygen burner. The crystal of $(BPy)_2Mo_2O_4F_6$ was accidentally obtained by hydrolysis during the crystal growth of $BPyMoOF_5$ in the same procedure as for the case of $EMImVOF_4$. Raman spectroscopy confirmed that major part of the sample that contained the crystal of $(BPy)_2Mo_2O_4F_6$ was still $BPyMoOF_5$.

X-ray Powder Diffraction: The sample was transferred into a quartz capillary under a dry Ar atmosphere as in the case of single-crystal diffraction. The sample was centered on an X-ray diffractometer (R-axis Rapid II, Rigaku) equipped with an imaging plate area detector (using the program RAPID XRD 2.3.3[50]) and graphite-monochromated Mo-K_α radiation (0.71073 Å). The ϕ angle was rotated at a rate of $1°s^{-1}$ and the ω and χ angles were fixed at 20° and 0°, respectively, during the collection (1000 s).

X-ray Single Crystal Diffraction: The single crystal of $EMImVOF_4$ used for data collection was a yellow transparent block measuring $0.2 \times 0.2 \times 0.3$ mm^3 and was centered on the diffractometer (R-axis Rapid II Rigaku with the imaging plate detector, controlled by the program RAPID AUTO 2.40[51]). Data collection was performed at 100 K and consisted of 12 ω scans (130–190°, 5° per frame) at fixed ϕ (0°) and χ (45°) angles and 32 ω scans (0–160°, 5° per frame) at fixed ϕ (180°) and χ (45°) angles. Crystal-to-detector distance was fixed at 127.4 mm. The exposure time was 30 s deg^{-1}. Integration, scaling, and absorption corrections were performed by using RAPID AUTO 2.40. The structure was solved by using SIR-92[52] and refined by SHELXL-97[53] linked to Win-GX.[54] Anisotropic displacement factors were introduced for all atoms except for hydrogen. The single crystal of $(BPy)_2Mo_2O_4F_6$ used for data collection was a yellow transparent block measuring $0.2 \times 0.2 \times 0.3$ mm^3. The data collection was carried out in the same manner as in the case for $EMImVOF_4$ with the exposure time of 180 s deg^{-1}. Crystallographic data and refinement results for $EMImVOF_4$ and $(BPy)_2Mo_2O_4F_6$ are given in Table 3. CCDC-753931 (for $EMImVOF_4$) and -753932 [for $(BPy)_2Mo_2O_4F_6$] contain the supplementary crystallographic data for this paper. These data can be obtained free of charge from The Cambridge Crystallographic Data Centre via www.ccdc.cam.ac.uk/data_request/cif.

Table 3. Summary of crystallographic data and refinement results for $EMImVOF_4$ and $(BPy)_2Mo_2O_4F_9$.

	[EMIm][VOF$_4$]	[BPy]$_2$[Mo$_2$O$_4$F$_6$]
Empirical formula	$C_6H_{11}F_4N_2OV$	$C_{18}H_{28}F_6Mo_2N_2O_4$
Formula weight	254.10	642.30
Crystal system	monoclinic	monoclinic
Space group	$P2_1/c$	$C2/c$
a [Å]	8.1909(3)	11.2713(2)
b [Å]	9.0218(8)	12.0769(3)
c [Å]	14.1098(4)	16.7409(3)
β [°]	104.9350(10)	95.5010(10)
V [Å^3]	1007.44(6)	2268.32(8)
Z	4	4
$d_{calcd.}$ [g cm^{-3}]	1.675	1.881
T [K]	100	100
R_1[a]	0.0225	0.0449
wR_2[b]	0.0634	0.1204

[a] $R_1 = \Sigma||F_o| - |F_c||/\Sigma|F_o|$. [b] $wR_2 = [\Sigma w[|F_o|^2 - |F_c|^2]^2/\Sigma w|F_o|^2]^{1/2}$.

Supporting Information (see footnote on the first page of this article): Raman and IR spectroscopic data; Walden plot for EMIm-based ILs; X-ray powder diffraction pattern; geometries of the interactions between the hydrogen atoms in the cation and fluorine or oxygen atoms in the anion.

[1] M. Gerken, H. P. A. Mercier, G. J. Schrobilgen in *Advanced Inorganic Fluorides* (Eds.: T. Nakajima, B. Zemva, A. Tressaud), Elsevier, New York, **2000**, p. 117–174.
[2] J. Darriet, W. Massa, J. Pebler, R. Stoef, *Solid State Sci.* **2002**, *4*, 1499–1508.
[3] L. Wang, Y. Li, *Chem. Mater.* **2007**, *19*, 727–734.
[4] K. Scheurell, G. Scholz, E. Kemmitz, *J. Solid State Chem.* **2007**, *180*, 749–758.
[5] A. Baiker, P. Dollenmeier, A. Reller, *J. Catal.* **1987**, *103*, 394–398.
[6] T. Ressler, J. Wienold, R. E. Jentoft, *J. Catal.* **2002**, *103*, 67–83.
[7] A. Butler, M. J. Clague, G. E. Meister, *Chem. Rev.* **1994**, *94*, 625–638.
[8] K. H. Thompson, J. H. McNeil, C. Orvig, *Chem. Rev.* **1999**, *99*, 2561–2572.
[9] D. C. Crans, *J. Inorg. Biochem.* **2000**, *80*, 123–131.
[10] D. C. Crans, J. J. Smee, E. Gaidamauskas, L. Yang, *Chem. Rev.* **2004**, *104*, 849–902.
[11] D. W. Aldous, R. J. Goff, J. P. Attfield, P. Lightfoot, *Inorg. Chem.* **2007**, *46*, 1277–1282.
[12] V. M. Schabergt, G. Pausewang, W. Massa, *Z. Anorg. Allg. Chem.* **1983**, *506*, 169–177.
[13] K. Waltersson, *J. Solid State Chem.* **1979**, *29*, 195–204.
[14] R. Mattes, H. Foerster, *J. Solid State Chem.* **1982**, *45*, 154–157.
[15] D. W. Aldous, N. F. Stephens, P. Lightfoot, *Dalton Trans.* **2007**, 2271–2282.
[16] D. W. Aldous, N. F. Stephens, P. Lightfoot, *Dalton Trans.* **2007**, 4207–4213.
[17] A. L. Bail, A. M. Mercier, I. Dix, *Acta Crystallogr., Sect. E* **2009**, *65*, i46–i47.
[18] J. A. S. Howell, K. C. Moss, *J. Chem. Soc. A* **1971**, *270*, 270–272.
[19] G. W. Bushnell, K. C. Moss, *Can. J. Chem.* **1972**, *50*, 3700–3705.
[20] S. Rostamzadehmansor, G. Ebrahimzadehrajaei, S. Ghammamy, K. Mehrani, L. Saghatforoush, *J. Fluorine Chem.* **2008**, *129*, 674–679.
[21] M. E. Welk, A. J. Norquist, C. L. Stern, K. R. Poeppelmeier, *Inorg. Chem.* **2000**, *39*, 3946–3947.
[22] R. R. Ryan, S. H. Mastin, M. J. Reisfeld, *Acta Crystallogr., Sect. B* **1971**, *27*, 1270–1274.
[23] R. Mattes, H. Förster, *J. Less-Common Met.* **1982**, *87*, 237–247.
[24] J. Swann, T. D. Westmoreland, *Inorg. Chem.* **1997**, *36*, 5348–5357.
[25] R. Mattes, K. Mennemann, N. Jäckel, H. Rieskamp, H. J. Brockmeyer, *J. Less-Common Met.* **1980**, *76*, 199–212.
[26] K. Adil, J. Marrot, M. Leblanc, V. Maisonneuve, *Acta Crystallogr., Sect. E* **2007**, *63*, m1511–m1513.
[27] V. A. Beuter, W. Sawodny, *Z. Anorg. Allg. Chem.* **1976**, *427*, 37–44.
[28] M. R. Marvel, R. A. F. Pinlac, J. Lesage, C. L. Stern, K. R. Poeppelmeier, *Z. Anorg. Allg. Chem.* **2009**, *635*, 869–877.
[29] J. E. Kirsch, H. K. Izumi, C. L. Stern, K. R. Poeppelmeier, *Inorg. Chem.* **2005**, *44*, 4586–4593.
[30] E. Burkholder, J. Zubieta, *Inorg. Chim. Acta* **2004**, *357*, 279–284.
[31] E. Burkholder, V. Golub, C. L. O'Connor, J. Zubieta, *Inorg. Chem.* **2004**, *43*, 7014–7029.
[32] K. R. Seddon, *J. Chem. Technol. Biotechnol.* **1997**, *68*, 351–356.

[33] T. Welton, *Chem. Rev.* **1999**, *99*, 2071–2083.
[34] P. Wasserscheid, W. Keim, *Angew. Chem. Int. Ed.* **2000**, *39*, 3772–3789.
[35] C. M. Gordon, *Appl. Catal. A* **2001**, *222*, 101–117.
[36] D. Zhao, M. Wu, Y. Kou, E. Min, *Catal. Today* **2002**, *74*, 157–189.
[37] J. Dupont, R. F. de Souza, P. A. Z. Suarez, *Chem. Rev.* **2002**, *102*, 3667–3692.
[38] C. E. Song, *Chem. Commun.* **2004**, 1033–1043.
[39] K. Matsumoto, R. Hagiwara, R. Yoshida, Y. Ito, Z. Mazej, P. Benkič, B. Žemva, O. Tamada, H. Yoshino, S. Matsubara, *Dalton Trans.* **2004**, 144–149.
[40] K. Matsumoto, R. Hagiwara, Z. Mazej, P. Benkič, B. Žemva, *Solid State Sci.* **2004**, *8*, 1250–1257.
[41] T. Kanatani, K. Matsumoto, R. Hagiwara, *Chem. Lett.* **2009**, *7*, 714–715.
[42] T. Kanatani, R. Ueno, K. Matsumoto, T. Nohira, R. Hagiwara, *J. Fluorine Chem.* **2009**, *130*, 979–984.
[43] K. Matsumoto, R. Hagiwara, *J. Fluorine Chem.* **2005**, *126*, 1095–1100.
[44] Y. Katayama, S. Dan, T. Miura, T. Kishi, *J. Electrochem. Soc.* **2001**, *148*, C102–C105.
[45] A. S. Wills, I. D. Brown, *VaList*, CEA, France, **1999**.
[46] N. E. Brese, M. O'Keeffe, *Acta Crystallogr., Sect. B* **1991**, *47*, 192–197.
[47] H. H. Paradies, F. Habben, *Acta Crystallogr., Sect. C* **1993**, *49*, 744–747.
[48] D. L. Ward, R. R. Rhinebarger, I. A. Popov, *Acta Crystallogr., Sect. C* **1986**, *42*, 1771–1773.
[49] R. Hagiwara, K. Matsumoto, Y. Nakamori, T. Tsuda, Y. Ito, H. Matsumoto, K. Momota, *J. Electrochem. Soc.* **2003**, *150*, D195–D199.
[50] *RAPID XRD*, version 2.3.3, Rigaku Corporation, Tokyo, Japan, **1999**.
[51] *RAPID XRD*, version 2.40, Rigaku Corporation, Tokyo, Japan, **2006**.
[52] A. Alomare, M. C. Burla, M. Camalli, G. Cascarano, C. Giacovazzo, A. Gugliardi, G. Polidori, *J. Appl. Crystallogr.* **1994**, *27*, 435.
[53] G. M. Sheldrick, *SHELX-97*, University of Göttingen, Germany, **1997**.
[54] L. J. Farrugia, *J. Appl. Crystallogr.* **1999**, *32*, 837–838.

Received: November 12, 2009
Published Online: January 19, 2010

